1
The Orbital Angular Momentum of Light: An Introduction

Les Allen and Miles Padgett

1.1
Introduction

Most physicists know that polarized light is associated with the spin angular momentum of the photon. It is almost certainly true that the idea of orbital angular momentum is a good deal less understood. Perhaps the simplest and most obvious display of both the spin and orbital angular momentum of light beams comes from an examination of the ratio of their angular momentum to their energy.

For an idealized, circularly-polarized plane wave, the spin angular momentum is given by $J_z = N\hbar$ and the energy by $W = N\hbar\omega$, where N is the number of photons. The angular momentum to energy ratio is thus,

$$\frac{J_z}{W} = \frac{\hbar}{\hbar\omega} = \frac{1}{\omega} \tag{1.1}$$

In fact the ratio in Eq. (1.1) is derivable from classical electromagnetism without any need to invoke the concept of a photon or any other quantum phenomenon [1].

A slightly more general result for elliptically polarized light, characterized by $-1 \leqslant \sigma \leqslant +1$, (with $\sigma = \pm 1$ for left- and right-handed circularly polarized light respectively and $\sigma = 0$ for linearly polarized light) is given by

$$\frac{J_z}{W} = \frac{\sigma}{\omega} \tag{1.2}$$

We can show for a light beam which has an l-dependent azimuthal phase angle such that the field amplitude is given by $u(x, y, z, \phi) = u_0(x, y, z)\, e^{-ikz} e^{+il\phi}$, that Eq. (1.2) becomes [2]

$$\frac{J'_z}{W} = \frac{l \pm \sigma}{\omega} \tag{1.3}$$

Here $\hbar\sigma$ describes the spin angular momentum per photon, while $l\hbar$ describes the orbital angular momentum per photon. In the absence of the phase term $\exp(il\phi)$, Eq. (1.3) would be the usual plane wave ratio of spin angular momentum divided by energy, namely, $\hbar\sigma/\hbar\omega$ or $\hbar\sigma$ per photon.

It transpires that this simple result is true both in the limit of the paraxial approximation and for fields described by a rigorous and unapproximated application of

Twisted Photons: Applications of Light with Orbital Angular Momentum.
Edited by Juan P. Torres and Lluis Torner

ISBN: 978-3-527-40907-5

Maxwell's equations [3]. In the paraxial approximation, other than assuming that $u(x, y, z)$ is normalizable and leads to a finite energy in the beam, no assumption has been made about the form of the distribution. In other words even for $\sigma = 0$, when the light is linearly polarized, there remains an angular momentum related to the spatial properties of the beam and dependent on l.

The fact that the simple paraxial result, Eq. (1.3), is fully justified by rigorous theory [4] enables a number of essentially simple conclusions to be drawn. The paraxial fields appropriate for linearly polarized light are

$$\mathbf{B} = \mu_0 \mathbf{H} = ik\left[u\hat{\mathbf{y}} + \frac{i}{k}\frac{\partial u}{\partial y}\hat{\mathbf{z}}\right]e^{ikz} \tag{1.4}$$

and

$$\mathbf{E} = ik\left[u\hat{\mathbf{x}} + \frac{i}{k}\frac{\partial u}{\partial x}\hat{\mathbf{z}}\right]e^{+ikz} \tag{1.5}$$

These allow evaluation of the time-averaged Poynting vector, $\varepsilon_0\, \mathbf{E} \times \mathbf{B}$, namely,

$$\begin{aligned}\varepsilon_0 \langle \mathbf{E} \times \mathbf{B} \rangle &= \frac{\varepsilon_0}{2}\left[\left\langle \mathbf{E}^* \times \mathbf{B} \right\rangle + \left\langle \mathbf{E} \times \mathbf{B}^* \right\rangle\right] \\ &= i\omega\frac{\varepsilon_0}{2}\left(u\nabla u^* - u^*\nabla u\right) + \omega k \varepsilon_0 |u|^2 \hat{\mathbf{z}}\end{aligned} \tag{1.6}$$

For a field such as $u(r, \phi, z) = u_0(r, z)\, e^{+il\phi}$ the ϕ-component of linear momentum density is

$$\varepsilon_0 \langle \mathbf{E} \times \mathbf{B} \rangle_\phi = \varepsilon_0 \omega l |u|^2 / r \tag{1.7}$$

while its cross product with r gives an angular momentum density of magnitude $j_z = \varepsilon_0 \omega \ell |u|^2$. The energy density of such a beam is

$$w = c\varepsilon_0 \langle \mathbf{E} \times \mathbf{B} \rangle_z = c\varepsilon_0 \omega k |u|^2 = \varepsilon_0 \omega^2 |u|^2 \tag{1.8}$$

Thus,

$$\frac{j_z}{w} = \frac{l}{\omega}$$

When the angular momentum density is integrated over the x–y plane, the ratio of angular momentum to energy per unit length of the beam is simply,

$$\frac{J_z}{W} = \frac{\iint r dr d\varphi \left(r \times \langle \mathbf{E} \times \mathbf{B} \rangle\right)_z}{c \iint r dr d\phi \langle \mathbf{E} \times \mathbf{B} \rangle_z} = \frac{l}{\omega} \tag{1.9}$$

The same straightforward calculation for fields that include polarization, again produces Eq. (1.3), but it is now for physically realizable fields and not just plane wave fields of infinite extent.

The earliest work on the orbital angular momentum of light beams took an LG (Laguerre–Gaussian) mode as the most easily available source of light possessing an azimuthal phase. This amplitude distribution, $u_{p,l}$, has the requisite $\exp(il\phi)$

term and is now well known. It readily follows for such a distribution that the linear momentum density is [2]

$$p = \varepsilon_0 \left(\frac{\omega k r z}{z_R^2 + z^2} \hat{\mathbf{r}} + \frac{\omega l}{r} \hat{\boldsymbol{\phi}} + \omega k \hat{\mathbf{z}} \right) \left| u_{p,l} \right|^2 \tag{1.10}$$

and the cross product with r gives the angular momentum density,

$$\mathbf{j} = \mathbf{r} \times \mathbf{p} = \varepsilon_0 \left(\frac{-\omega l z}{r} \hat{\mathbf{r}} - \omega k r \left(\frac{z_R^2}{z_R^2 + z^2} \right) \hat{\boldsymbol{\phi}} + \omega l \hat{\mathbf{z}} \right) \left| u_{p,l} \right|^2 \tag{1.11}$$

The expression for linear momentum p, (Eq. (1.10)), shows that at a constant radius, r, the Poynting vector maps out a spiral path of well-defined pitch,

$$z_p = \frac{2\pi k r^2}{l} \tag{1.12}$$

However, such a picture is misleading as it ignores the radial component of the Poynting vector and, hence, the spreading of the beam upon propagation [5]. For constant $r(z)/w(z)$, the angle of rotation, θ, of the Poynting vector from the beam waist at $z = 0$ is

$$\theta = \frac{l}{2} \left(\frac{w(z)}{r(z)} \right)^2 \arctan \left(\frac{z}{z_R} \right) \tag{1.13}$$

For a $p = 0$ mode, for which the intensity distribution is a single ring, the radius of the maximum amplitude in the mode is given by

$$r(z)_{\text{Max Int.}} = \sqrt{\frac{w(z)\, l}{2}} \tag{1.14}$$

and so for $p = 0, \ell \neq 0$, it follows that $\theta = \arctan\left(\frac{z}{z_R}\right)$ which, surprisingly, is independent of ℓ. Rather than describing a multiturn spiral as one might have presumed, the Poynting vector rotates only by $\pi/2$ either side of the beam waist as the light propagates to the far field. Perhaps even more surprisingly, the locus of the vector is simply a straight line at an angle to the axis of the beam [6, 7]. Note that the arctan term is simply proportional to the Gouy phase of the Gaussian beam and that, in free space, the Poynting vector is at all points parallel to the wavevector.

Simple though these results are, in hindsight, they were not known until the early 1990s. Their application to a number of conceptually straightforward experiments enables simple comparisons to be made, at least in the paraxial regime, between the behavior of spin and orbital angular momenta and enables the observation of a number of phenomena to be elucidated. This phenomenology provides much of the basis for the exploration and exploitation of the current understanding of the subject outlined in later chapters of this book. Although everything may be justified formally using a quantum approach, there is, outside of entanglement, little need to leave this classical formulation. In the nonparaxial case, the separation of spin and orbital angular momentum is more complicated [4, 8–10].

The use of the flow of angular momentum flux across a surface, rather than angular momentum density, allows the separation of the spin and orbital angular momentum parts in a gauge invariant way. This holds beyond the paraxial approach

but confirms the simple values obtained for the ratio of angular momentum to energy [11].

1.2 The Phenomenology of Orbital Angular Momentum

Simple comparisons of the behavior of spin and orbital angular momenta in different situations prove to be a fruitful way to demonstrate their properties. First, however, we need to distinguish the general structures of light emitted by a laser and also its properties when converted to, for instance, an LG beam. Laser beams usually have spherical wave fronts while the azimuthal phase leads to beams with l intertwined helical wave fronts (Figure 1.1). The LG beam is not the only example of a helical wave front; Bessel beams [12], Mathieu beams [13], and Ince–Gaussian beams [14] can also carry orbital angular momentum. In all cases, the interference of these helical wave fronts with a plane wave gives rise to characteristic spiral interference fringes [15–17].

The production of a pure, high-order LG mode from a laser beam was first achieved using a mode convertor based on cylindrical lenses [18]. Although the details are interesting, they need not concern us here, as an approach based on simple holograms achieves a similar beam much more easily. Prior to the generation of LG beams with lenses, similar beams containing the same azimuthal phase term had also been produced using diffractive optical elements [19]. These components are simple diffraction gratings, that contain an edge dislocation,

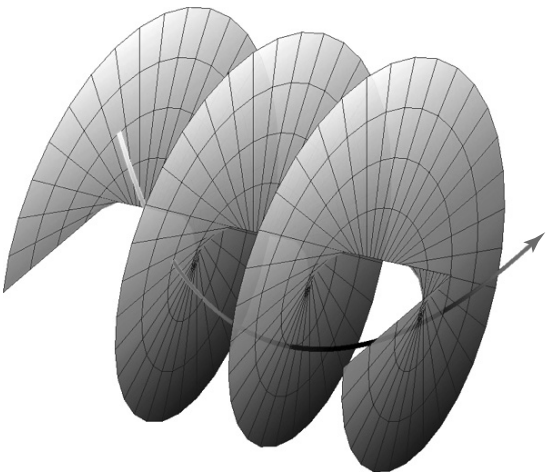

Figure 1.1 The helical wave fronts characterized by an azimuthal phase term ($l = 1$) and the associated Poynting vector, the azimuthal component of which gives rise to an orbital angular momentum. (Please find a color version of this figure on the color plates.)

coincident with the axis of the illuminating beam. Such ''forked-gratings'' give rise to a first order diffracted spot with an annular intensity cross section, which is a natural consequence of the $\exp(il\phi)$ phase structure. Indeed, similar beams have been widely studied as examples of optical phase singularities [20], also called *optical vortices* [21, 22]. However, in none of the earlier works had their angular momentum properties been recognized. These diffractive optical components can be readily designed, and are frequently referred to as *computer generated holograms*. Although easy to implement and producing perfect helical wave fronts, the resulting intensity distribution only approximates to that of a pure LG mode. Most recently, these ''forked diffraction gratings'' have been employed within the image train of a microscope to impose a point-spread function corresponding to a helical mode, giving an edge enhancement of the image [23, 24].

Rather than using the diffractive optical component, it is possible to form a refractive optical equivalent. A spiral phaseplate has an optical thickness, t, given by $t = \lambda l\phi/2\pi$, where ϕ is the azimuthal angle [25]. Upon transmission, a plane wave input beam is transformed into a helically phased beam again characterized by an azimuthal phase structure of $\exp(il\phi)$. Such spiral phase plates are not easy to manufacture but offer very high conversion efficiency. Interestingly, the azimuthal refraction of the ramped surface gives a skew angle of l/kr to each transmitted ray. For the linear momentum of the photon of $\hbar k$, this gives an azimuthal component $l\hbar/r$ and hence an angular momentum of $l\hbar$ per photon [26]. Thus we see that for a ray optical model, the orbital angular momentum of the photon is describable by skew rays [27].

Despite the various approaches that have been developed to generate helically phased beams, they are not a feature unique to advanced optical experiment. Interference between two plane waves yields sinusoidal fringes. Interference between three [28] or more [29] plane waves leads to points within the field cross section of perfect destructive interference around which the phase advances or retards by 2π. Nowhere is this more apparent than when examining the optical speckle resulting from laser light being scattered from a rough surface, where each black speck is a perfect phase singularity. Of course, the specks are dark and hence carry neither energy nor momentum. However, the light in the immediate vicinity of each is characterized by a helical phase front and does carry both energy and orbital angular momentum. Over the extent of the speckle pattern, there are an equal number of clockwise and anticlockwise singularities; and hence the overall orbital angular momentum tends to zero. These phase singularities map out lines of complete darkness in space, with both fractal [30] and topological [31] properties.

In order to generate pure LG modes, the cylindrical lens mode converter remains a convenient approach. The fidelity of the mode transformation means that when light with orbital angular momentum is passed through a cylindrical lens mode convertor it behaves in a mathematically analogous way to polarized (spin) light through a quarter waveplate. Indeed, the representation of states on the Poincaré sphere can be applied for any two states of orbital angular momentum [32]. Similarly, the well-known Jones matrices which describe the propagation of polarized light through an optical system have equivalents for the propagation of orbital angular momentum

through a system with astigmatic optical elements [33, 34]. There are also joint matrices for light that is both polarized and possesses orbital angular momentum. An alternative to the use of these joint matrices is to apply the spin (Jones) matrix and then the orbital angular momentum matrix separately. This is equivalent to the separation of the spin and orbital components in the hydrogen wavefunction.

That this orbital angular momentum is a true momentum was first demonstrated in optical tweezers [35]. Optical tweezers use the gradient force associated with a tightly focused beam of the light to trap a microscopic dielectric particle [36]. A few milliwatts is all that is required to trap a 5 μm diameter sphere suspended in a liquid medium. Using an LG mode as the trapping beam results in a transfer of angular momentum to the particle causing it to spin about the beam axis.

The similarities in behavior of the two types of angular momenta in a light beam are also shown in optical tweezers when a small, mildly absorptive particle is trapped *on-axis*. When the light is purely circularly polarized, the particle may be made to rotate clockwise or anticlockwise depending on the handedness of the polarization where $\sigma = \pm 1$. When the same trapped particle sees light with $l = \pm 1$, it can also be made to rotate in either direction. Application of light where σ and l have the same sign leads to a faster rotation proportional to $(\sigma + l)$, while if σ and l have opposite signs the particle slows to a halt which arises clearly from $(\sigma - l)$. This demonstrates the mechanical equivalence of spin and orbital angular momentum [37]. In other words, the spin angular momentum can be added to or subtracted from the orbital component, consistent with the statement that the optical angular momentum of a light beam is $(l + \sigma)\hbar$. This statement is in agreement with the theory of angular momentum flux. It is observed that the center of mass in the on-axis case does not move and both the spin and orbital angular momentum contribute to making the sphere rotate about its own axis. *Off-axis*, such a particle behaves rather differently. It responds to orbital angular momentum by orbiting the axis of the beam with an angular velocity proportional to the local intensity of the beam. It also spins, because of σ, about its own axis. Again the velocity depends on the local intensity but otherwise spin and orbital manifest themselves in that case in different ways – highlighting the intrinsic and extrinsic nature of optical angular momentum [38]. These various studies in optical tweezers have spawned significant work, worldwide, where the induced rotation of the particles acts as a microfluidic pump [39, 40] or other optically driven micromachine [41–44].

It should be observed that spin, σ, is said to be *intrinsic* because it is independent of the choice of axis about which it is calculated. However, orbital, l, depends upon the choice of axis. Nevertheless, when there is a direction, z, for which the transverse linear momentum of the beam is zero, both l and σ are invariant under a shift of axis and the orbital component might be said to be *quasi-intrinsic*. For off-axis apertures in cylindrically symmetric beams the transverse linear momentum is nonzero and l is *extrinsic*.

Closely related to the use of LG beam in optical tweezers is their interaction with cold atoms [45]. In many cases, rather than the helical wave fronts, it is the on-axis intensity zero that enables the confinement of blue-detuned atoms

[46]. Residual scattering can additionally lead to guiding along the length of the singularity. Cooling the atoms further to create a Bose–Einstein condensate (BEC) results in yet more interesting interactions between matter and the orbital angular momentum of light. This includes an optically induced rotation of the BEC [47, 48].

The interaction of light carrying orbital angular momentum with an in resonance atom has also been investigated [49]. It is found that the frequency shift of a resonant transition in an atom moving with an angular velocity Ω through a polarized beam with orbital angular momentum is Ωl while the torque on the center of mass of the atom is $\hbar l\Gamma$ and independent of σ [50]. There appear to be no torques on the atom's center of mass that depend on $(l+\sigma)$.

This frequency shift is an example of an angular Doppler effect readily observed when a light beam is rotated at angular frequency Ω about its own axis. This is not to be confused with the transverse Doppler shift observed when an emitter moves toward or away from the source. For the spinning beam, the frequency of the light is shifted for spin by $\delta\omega' = \Omega\sigma$, for orbital angular momentum by $\delta\omega'' = \Omega l$ [51] and for total angular momentum by $\delta\omega''' = \Omega(\sigma + l)$ [52]. For combined beams with the same polarization but different total orbital angular momenta, a spectrum of shifted components $\delta\omega_1 = \Omega(\sigma + l_1)$, $\delta\omega_2 = (\sigma + l_2)$, and so on, is produced. This is one of the effects found to depend upon the sum of the spin and orbital components. The phenomenon can be understood by the realization that time evolution of a helical phase front is indistinguishable from rotation about the beam axis. A full rotation of the beam changes the phase of the light by $l + \sigma$ cycles. Such phase and associated frequency shifts also extend to polychromatic light, where all spectral components are frequency shifted by the same amount [53].

Attempts have been made to see if analogs to electron spin-orbit interactions common in atoms exists in light. The only evidence so far is that in the dissipative force on a moving atom there is a term proportional to σl. It is, however, small and only comparable in size to terms which are usually ignored, of order $(1/k^2)$ [54].

Second harmonic generation or up-conversion in a nonlinear crystal can produce second harmonic generation for helically phased modes, where

$$\omega_{\mathrm{Shg}} = \omega_{\mathrm{In}} + \omega_{\mathrm{In}} = 2\omega_{\mathrm{In}} \text{ and } l_{\mathrm{Shg}} = l_{\mathrm{In}} + l_{\mathrm{In}} = 2l_{\mathrm{In}} \tag{1.15}$$

This is in contrast to the spin angular momentum which can only be unity, at most. Here, there is another difference between orbital and spin angular momentum. There is no potential upper bound to l_{Shg} and we see that up-conversion may be used to change the order of the mode [55]. There is no equivalent change of polarization mode. This conversion of l_{Shg} arises through strict phase matching and because the wavevectors and Poynting vector of the fundamental and second-harmonic helical beams are collinear. This implies that when the wave-number doubles then l must also double [56]. Such a process is consistent with the conservation of orbital angular momentum within the light fields. This work is a precursor of work on down-conversion where one input photon creates two photons of lower energy. This has important implications for the higher order entanglement possible with orbital angular momentum [57]. In down-conversion, correlation of orbital angular momentum can be achieved with a pair of holograms that determine l_{Idler} and

l_{Signal} for a given l_{Pump} [58, 59]. Although spin is limited to ± 1, there is a wide range of l_{Idler} and l_{Signal} for a given l_{Pump}. The high-dimensionality of the Hilbert space and information content [60] combined with techniques for sorting single photons [61–63] creates opportunities in, for example, quantum information processing [64]. It is the study of the down converted beams and a violation of a Bell inequality [65] that illustrates that orbital angular momentum is a meaningful concept at the quantum level and hence a true photon property.

For spin angular momentum and circularly polarized light, the light source need not be either temporally or spatially coherent. For orbital angular momentum the situation is more complicated. Orbital angular momentum is a meaningful concept across the full electromagnetic spectrum [66] and has been considered ranging from radio frequency [67] to X ray regimes [68]. As orbital angular momentum is associated with the phase cross section of the beam, there is no restriction on its temporal coherence; each spectral component can have a perfect $\exp(-il\phi)$ phase structure. Beams with such multispectral components can be generated using the normal forked diffraction grating, but with its spectral dispersion compensated by a prism [69] or second grating [70]. These beams have the exact anticipated orbital angular momentum to cause microscopic objects to rotate about the axis of the beam [71]. Perfect helical wave fronts imply a complete spatial coherence. Degrading the spatial coherence destroys the fidelity of the on-axis phase singularity and the on-axis intensity zero. If the beam has some degree of spatial coherence then when transmitted through a spiral phase plate or diffracted from a forked diffraction grating, the resulting beam can be decomposed into an incoherent sum of different modes having a finite average value of orbital angular momentum. These beams have been termed *Rankine vortices* [72]. Spiral phaseplates built into telescopes have been shown to be useful astronomical filters, which could suppress the light from a point-star so that an off-axis source of light from a planet might be detected [73, 74].

Another aspect of clear distinction between spin and orbital angular momentum is the existence of a Fourier relationship for orbital angular momentum and angular position [75], and a related uncertainty relationship. The uncertainty relationship was originally discussed for measurements of linear position and linear momentum. In the case of orbital angular momentum, a similar expression can be written for small uncertainties in angular position, $\Delta\phi\Delta l = \hbar/2$ [76]. No equivalent expression exists for spin. The uncertainty associated with the measurement of orbital angular momentum may prove to be a limitation to the evident virtues of orbital angular momentum as a means of exploiting entanglement, and so on.

One marked difference in the literature, since light beams possessing orbital angular momentum have been realized and understood, arises because, in order to exploit their dependence on space, the formal way in which light interacts with atoms has had to be developed. It is no longer sufficient to investigate the interaction of atoms with plane waves. The traditional semiclassical approach is still in the main appropriate, but it must now be applied to specifically structured Gaussian beams.

Various reviews have been written, which summarize the development of the field of the last 15 years [3, 77–80] and many aspects of the current state of this work is discussed in later chapters of this book.

References

1. Poynting, J.H. (1909) The wave motion of a revolving shaft, and a suggestion as to the angular momentum in a beam of circularly polarised light. *Proc. R. Soc. London Ser. A*, **82**, 560–567.
2. Allen, L., Beijersbergen, M.W., Spreeuw, R.J.C., and Woerdman, J.P. (1992) Orbital angular momentum of light and the transformation of Laguerre-Gaussian laser modes. *Phys. Rev. A*, **45**, 8185–8189.
3. Allen, L., Padgett, M.J., and Babiker, M. (1999b) *The Orbital Angular Momentum of Light*, Progress in Optics, vol. XXXIX, Elsevier Science Publishers B V, Amsterdam.
4. Barnett, S.M. and Allen, L. (1994) Orbital angular momentum and nonparaxial light beams. *Opt. Commun.*, **110**, 670–678.
5. Padgett, M.J. and Allen, L. (1995) The Poynting vector in Laguerre-Gaussian laser modes. *Opt. Commun.*, **121**, 36–40.
6. Courtial, J. and Padgett, M.J. (2000) Limit to the orbital angular momentum per unit energy in a light beam that can be focussed onto a small particle. *Opt. Commun.*, **173**, 269–274.
7. Berry, M.V. and McDonald, K.T. (2008) Exact and geometrical optics energy trajectories in twisted beams. *J. Opt. A: Pure Appl. Opt.*, **10**, 7.
8. Ganic, D., Gan, X.S., and Gu, M. (2003) Focusing of doughnut laser beams by a high numerical-aperture objective in free space. *Opt. Express*, **11**, 2747–2752.
9. Monteiro, P.B., Neto, P.A.M., and Nussenzveig, H.M. (2009) Angular momentum of focused beams: beyond the paraxial approximation. *Phys. Rev. A*, **79**, 033830.
10. Nieminen, T.A., Stilgoe, A.B., Heckenberg, N.R., and Rubinsztein-Dunlop, H. (2008) Angular momentum of a strongly focused Gaussian beam. *J. Opt. A: Pure Appl. Opt.*, **10**, 6.
11. Barnett, S.M. (2002) Optical angular momentum flux. *J. Opt. B: Quantum Semiclassical Opt.*, **4**, S7–S16.
12. McGloin, D. and Dholakia, K. (2005) Bessel beam: diffraction in a new light, contemporary. *Physics*, **46**, 15–28.
13. Gutierrez-Vega, J.C., Iturbe-Castillo, M.D., and Chavez-Cerda, S. (2000) Alternative formulation for invariant optical fields: Mathieu beams. *Opt. Lett.*, **25**, 1493–1495.
14. Bandres, M.A. and Gutierrez-Vega, J.C. (2004) Ince-Gaussian beams. *Opt. Lett.*, **29**, 144–146.
15. Harris, M., Hill, C.A., and Vaughan, J.M. (1994) Optical helices and spiral interference fringes. *Opt. Commun.*, **106**, 161–166.
16. Padgett, M., Arlt, J., Simpson, N., and Allen, L. (1996) An experiment to observe the intensity and phase structure of Laguerre-Gaussian laser modes. *Am. J. Phys.*, **64**, 77–82.
17. Soskin, M.S., Gorshkov, V.N., Vasnetsov, M.V., Malos, J.T., and Heckenberg, N.R. (1997) Topological charge and angular momentum of light beams carrying optical vortices. *Phys. Rev. A*, **56**, 4064–4075.
18. Beijersbergen, M.W., Allen, L., van der Veen, H., and Woerdman, J.P. (1993) Astigmatic laser mode converters and transfer of orbital angular momentum. *Opt. Commun.*, **96**, 123–132.
19. Bazhenov, V.Y., Vasnetsov, M.V., and Soskin, M.S. (1990) Laser beams with screw dislocations in their wave-fronts. *JETP Lett.*, **52**, 429–431.
20. Nye, J.F. and Berry, M.V. (1974) Dislocation in wave trains. *Proc. R. Soc. London Ser. A: Math. Phys. Eng. Sci.*, **336**, 165–190.

21. Coullet, P., Gil, L., and Rocca, F. (1989) Optical vortices. *Opt. Commun.*, **73**, 403–408.
22. Desyatnikov, A.S., Kivshar, Y.S., and Torner, L. (2005) *Optical Vortices and Vortex Solitons*, Progress in Optics, Vol. 47, Elsevier Science Publishers B V, Amsterdam.
23. Furhapter, S., Jesacher, A., Bernet, S., and Ritsch-Marte, M. (2005) Spiral interferometry. *Opt. Lett.*, **30**, 1953–1955.
24. Bernet, S., Jesacher, A., Furhapter, S., Maurer, C., and Ritsch-Marte, M. (2006) Quantitative imaging of complex samples by spiral phase contrast microscopy. *Opt. Express*, **14**, 3792–3805.
25. Beijersbergen, M.W., Coerwinkel, R.P.C., Kristensen, M., and Woerdman, J.P. (1994) Helical-wave-front laser-beams produced with a spiral phaseplate. *Opt. Commun.*, **112**, 321–327.
26. Turnbull, G.A., Robertson, D.A., Smith, G.M., Allen, L., and Padgett, M.J. (1996) Generation of free-space Laguerre-Gaussian modes at millimetre-wave frequencies by use of a spiral phaseplate. *Opt. Commun.*, **127**, 183–188.
27. Leach, J., Keen, S., Padgett, M.J., Saunter, C., and Love, G.D. (2006b) Direct measurement of the skew angle of the Poynting vector in a helically phased beam. *Opt. Express*, **14**, 11919–11924.
28. Masajada, J. and Dubik, B. (2001) Optical vortex generation by three plane wave interference. *Opt. Commun.*, **198**, 21–27.
29. O'Holleran, K., Padgett, M.J., and Dennis, M.R. (2006) Topology of optical vortex lines formed by the interference of three, four, and five plane waves. *Opt. Express*, **14**, 3039–3044.
30. O'Holleran, K., Dennis, M., Flossmann, F., and Padgett, M.J. (2008) Fractality of light's darkness. *Phys. Rev. Lett.*, **100**, 053902.
31. O'Holleran, K., Dennis, M., and Padgett, M. (2009) Topology of Light's Darkness. *Phys. Rev. Lett.*, **102**, 143902.
32. Padgett, M.J. and Courtial, J. (1999) Poincare-sphere equivalent for light beams containing orbital angular momentum. *Opt. Lett.*, **24**, 430–432.
33. Allen, L., Courtial, J., and Padgett, M.J. (1999a) Matrix formulation for the propagation of light beams with orbital and spin angular momenta. *Phys. Rev. E*, **60**, 7497–7503.
34. Allen, L. and Padgett, M. (2007) Equivalent geometric transformations for spin and orbital angular momentum of light. *J. Mod. Opt.*, **54**, 487–491.
35. He, H., Friese, M.E.J., Heckenberg, N.R., and Rubinszteindunlop, H. (1995) Direct observation of transfer of angular-momentum to absorptive particles from a laser-beam with a phase singularity. *Phys. Rev. Lett.*, **75**, 826–829.
36. Ashkin, A., Dziedzic, J.M., Bjorkholm, J.E., and Chu, S. (1986) Observation of a single-beam gradient force optical trap for dielectric particles. *Opt. Lett.*, **11**, 288–290.
37. Simpson, N.B., Dholakia, K., Allen, L., and Padgett, M.J. (1997) Mechanical equivalence of spin and orbital angular momentum of light: an optical spanner. *Opt. Lett.*, **22**, 52–54.
38. O'neil, A.T., Macvicar, I., Allen, L., and Padgett, M.J. (2002) Intrinsic and extrinsic nature of the orbital angular momentum of a light beam. *Phys. Rev. Lett.*, **88**, 053601.
39. Ladavac, K. and Grier, D.G. (2004) Microoptomechanical pumps assembled and driven by holographic optical vortex arrays. *Opt. Express*, **12**, 1144–1149.
40. Leach, J., Mushfique, H., Di Leonardo, R., Padgett, M., and Cooper, J. (2006) An optically driven pump for microfluidics. *Lab Chip*, **6**, 735–739.
41. Galajda, P. and Ormos, P. (2001) Complex micromachines produced and driven by light. *Appl. Phys. Lett.*, **78**, 249–251.
42. Paterson, L., Macdonald, M.P., Arlt, J., Sibbett, W., Bryant, P.E., and Dholakia, K. (2001) Controlled rotation of optically trapped microscopic particles. *Science*, **292**, 912–914.
43. Grier, D.G. (2003) A revolution in optical manipulation. *Nature*, **424**, 810–816.
44. Knoner, G., Parkin, S., Nieminen, T.A., Loke, V.L.Y., Heckenberg, N.R., and

Rubinsztein-Dunlop, H. (2007) Integrated optomechanical microelements. *Opt. Express*, **15**, 5521–5530.

45. Barreiro, S. and Tabosa, J.W.R. (2003) Generation of light carrying orbital angular momentum via induced coherence grating in cold atoms. *Phys. Rev. Lett.*, **90**, 133001.
46. Ozeri, R., Khaykovich, L., and Davidson, N. (1999) Long spin relaxation times in a single-beam blue-detuned optical trap. *Phys. Rev. A*, **59**, R1750–R1753.
47. Andersen, M.F., Ryu, C., Clade, P., Natarajan, V., Vaziri, A., Helmerson, K., and Phillips, W.D. (2006) Quantized rotation of atoms from photons with orbital angular momentum. *Phys. Rev. Lett.*, **97**, 170406.
48. Wright, K.C., Leslie, L.S., and Bigelow, N.P. (2008) Optical control of the internal and external angular momentum of a Bose-Einstein condensate. *Phys. Rev. A*, **77**, 041601.
49. Allen, L., Babiker, M., Lai, W.K., and Lembessis, V.E. (1996) Atom dynamics in multiple Laguerre-Gaussian beams. *Phys. Rev. A*, **54**, 4259–4270.
50. Allen, L., Babiker, M., and Power, W.L. (1994) Azimuthal Doppler-shift in light-beams with orbital angular-momentum. *Opt. Commun.*, **112**, 141–144.
51. Courtial, J., Dholakia, K., Robertson, D., Allen, L., and Padgett, M.J. (1998) Measurement of the rotational frequency shift imparted to a rotating light beam possessing orbital angular momentum. *Phys. Rev. Lett.*, **80**, 3217–3219.
52. Courtial, J., Robertson, D., Dholakia, K., Allen, L., and Padgett, M.J. (1998) Rotational frequency shift of a light beam. *Phys. Rev. Lett.*, **81**, 4828–4830.
53. Nienhuis, G. (2006) Polychromatic and rotating beams of light. *J. Phys. B*, **39**, S529–S544.
54. Allen, L., Lembessis, V.E., and Babiker, M. (1996b) Spin-orbit coupling in free-space Laguerre-Gaussian light beams. *Phys. Rev. A*, **53**, R2937–R2939.
55. Dholakia, K., Simpson, N.B., Padgett, M.J., and Allen, L. (1996) Second-harmonic generation and the orbital angular momentum of light. *Phys. Rev. A*, **54**, R3742–R3745.
56. Courtial, J., Dholakia, K., Allen, L., and Padgett, M.J. (1997b) Second-harmonic generation and the conservation of orbital angular momentum with high-order Laguerre-Gaussian modes. *Phys. Rev. A*, **56**, 4193–4196.
57. Arnaut, H.H. and Barbosa, G.A. (2000) Orbital and intrinsic angular momentum of single photons and entangled pairs of photons generated by parametric down-conversion. *Phys. Rev. Lett.*, **85**, 286–289.
58. Mair, A., Vaziri, A., Weihs, G., and Zeilinger, A. (2001) Entanglement of the orbital angular momentum states of photons. *Nature*, **412**, 313–316.
59. Oemrawsingh, S.S.R., Ma, X., Voigt, D., Aiello, A., Eliel, E.R.T., Hooft, G.W., and Woerdman, J.P. (2005) Experimental demonstration of fractional orbital angular momentum entanglement of two photons. *Phys. Rev. Lett.*, **95**, 240501.
60. Gibson, G., Courtial, J., Padgett, M.J., Vasnetsov, M., Pas'ko, V., Barnett, S.M., and Franke-Arnold, S. (2004) Free-space information transfer using light beams carrying orbital angular momentum. *Opt. Express*, **12**, 5448–5456.
61. Leach, J., Courtial, J., Skeldon, K., Barnett, S.M., Franke-Arnold, S., and Padgett, M.J. (2004) Interferometric methods to measure orbital and spin, or the total angular momentum of a single photon. *Phys. Rev. Lett.*, **92**, 013601.
62. Marrucci, L., Manzo, C., and Paparo, D. (2006) Optical spin-to-orbital angular momentum conversion in inhomogeneous anisotropic media. *Phys. Rev. Lett.*, **96**, 163905.
63. Deng, L.P., Wang, H.B., and Wang, K.G. (2007) Quantum CNOT gates with orbital angular momentum and polarization of single-photon quantum logic. *J. Opt. Soc. Am. B: Opt. Phys.*, **24**, 2517–2520.
64. Molina-Terriza, G., Torres, J.P., and Torner, L. (2002) Management of the angular momentum of light: preparation of photons in multidimensional vector states of angular momentum. *Phys. Rev. Lett.*, **88**, 013601.
65. Leach, J., Jack, B., Romero, J., Ritsch-Marte, M., Boyd, R.W., Jha, A.K., Barnett, S.M., Franke-Arnold, S.,

and Padgett, M.J. (2009) Violation of a Bell inequality in two-dimensional orbital angular momentum state-spaces. *Opt. Express*, **17**, 8287–8293.
66. Harwit, M. (2003) Photon orbital angular momentum in astrophysics. *Astrophys. J.*, **597**, 1266–1270.
67. Thide, B., Then, H., Sjoholm, J., Palmer, K., Bergman, J., Carozzi, T.D., Istomin, Y.N., Ibragimov, N.H., and Khamitova, R. (2007) Utilization of photon orbital angular momentum in the low-frequency radio domain. *Phys. Rev. Lett.*, **99**, 087701.
68. Sasaki, S. and Mcnulty, I. (2008) Proposal for generating brilliant x-ray beams carrying orbital angular momentum. *Phys. Rev. Lett.*, **100**, 124801.
69. Leach, J. and Padgett, M.J. (2003) Observation of chromatic effects near a white-light vortex. *New J. Phys.*, **5**, 7.
70. Mariyenko, I.G., Strohaber, J., and Uiterwaal, C. (2005) Creation of optical vortices in femtosecond pulses. *Opt. Express*, **13**, 7599–7608.
71. Wright, A., Girkin, J., Gibson, G.M., Leach, J., and Padgett, M.J. (2008) Transfer of orbital angular momentum from a super-continuum, white-light beam. *Opt. Express*, **16**, 9495–9500.
72. Swartzlander, G.A. and Hernandez-Aranda, R.I. (2007) Optical Rankine vortex and anomalous circulation of light. *Phys. Rev. Lett.*, **99**, 160901.
73. Foo, G., Palacios, D.M., and Swartzlander, G.A. (2005) Optical vortex coronagraph. *Opt. Lett.*, **30**, 3308–3310.
74. Lee, J.H., Foo, G., Johnson, E.G., and Swartzlander, G.A. (2006) Experimental verification of an optical vortex coronagraph. *Phys. Rev. Lett.*, **97**, 053901.
75. Yao, E., Franke-Arnold, S., Courtial, J., Barnett, S., and Padgett, M.J. (2006) Fourier relationship between angular position and optical orbital angular momentum. *Opt. Express*, **14**, 9071–9076.
76. Franke-Arnold, S., Barnett, S., Yao, E., Leach, J., Courtial, J., and Padgett, M.J. (2004) Uncertainty principle for angular position and angular momentum. *New J. Phys.*, **6**, 103.
77. Allen, L., Barnett, S.M., and Padgett, M.J. (2003) *Optical Angular Momentum*, IoP Publishing. ISBN-0 7503 0901 6.
78. Padgett, M., Courtial, J., and Allen, L. (2004) Light's orbital angular momentum. *Phys. Today*, **57**, 35–40.
79. Molina-Terriza, G., Torres, J.P., and Torner, L. (2007) Twisted photons. *Nat. Phys.*, **3**, 305–310.
80. Franke-Arnold, S., Allen, L., and Padgett, M. (2008) Advances in optical angular momentum. *Laser Photonics Rev.*, **2**, 299–313.